Failure Modes and Mitigation Strategies for a Turboelectric Aircraft Concept with Turbine Electrified Energy Management

Jonathan L. Kratz[1] and Donald L. Simon[2]

NASA Glenn Research Center, Cleveland, Ohio, 44135, U.S.A.

The electrification of gas turbine engines represents a major step-change in aircraft propulsion systems commonly known as Electrified Aircraft Propulsion (EAP). EAP involves the integration of electric machines potentially functioning as generators for large-scale power extraction, as motors providing electrical augmentation of the engine spools, and even as a means of driving propulsors beyond the immediate scope of the engine. It may also include the use of energy storage. These and other characteristics of hybrid electric propulsion systems are relatively new to aircraft propulsion. The expanded propulsion architecture can be leveraged to improve propulsive efficiency and achieve better vehicle aerodynamics and controllability. It can also allow for additional benefits such as those enabled through Turbine Electrified Energy Management (TEEM). As the propulsion system and its functions expand, new failure modes are introduced. Due to the highly coupled nature of the propulsion system, failures could propagate throughout the system in ways that are unique to the new EAP architectures. To build confidence in the safety and practicality of EAP concepts, these failure modes need to be identified, explored, and addressed through mitigation strategies. This paper seeks to evaluate failure modes and failure mitigation strategies for the EAP concept known as the Single-aisle Turboelectric AiRCaft with Aft Boundary Layer propulsor (STARC-ABL). The TEEM control concept is applied to improve transient operability. Several failure modes are considered and control-based failure mitigation strategies are proposed with the goal of retaining operability and overall thrust. The results demonstrate the ability to maintain operability and a substantial amount of thrust in the event of various types of failures. Some challenges are also identified and discussed.

Nomenclature

English Variables

N	=	rotational speed, rpm
N_c	=	corrected rotational speed, rpm
P	=	power, hp
P_{avail}	=	electric power available to the tail cone thruster based on the corrected speeds of GTF1 and GTF2
P_{frac}	=	fraction of the overall power extraction that is extracted from the HPS. The remainder is from the LPS.
PLA	=	power lever angle, degrees
p_{s3}	=	static pressure at the HPC exit, psi
SM	=	stall margin, %
SOC	=	state of charge, %
state	=	value signifies if the engine is accelerating, decelerating, or experiencing steady-state operation
T_2	=	total temperature at the inlet of the fan, °R
T_4	=	total temperature at the inlet of the HPT, °R

---

[1] Research Engineer, Intelligent Control & Autonomy Branch, AIAA member.
[2] Research Engineer, Intelligent Control & Autonomy Branch, non-AIAA member.

taper   =   value by which the transient EM power command is multiplied to facilitate a smooth transition to steady state operation

VAFN =   variable area fan nozzle, in^2

VBV   =   variable bleed valve, fraction

W_c =   corrected flow rate, lb_m/s

W_f =   fuel flow rate, lb_m/s

Greek Variables

Δ =   change in the variable value

τ =   torque, ft-lb_f

Subscripts

dmd   =   controller demand

EM1   =   Electric Machine 1 – derives its power from GTF1

EM2   =   Electric Machine 2 – derives its power from GTF2

fan   =   corresponds to the fan of the relevant component (GTF or TCT)

GTF1   =   corresponds to geared turbofan 1

GTF2   =   corresponds to geared turbofan 2

HPS   =   corresponds to the HPS

HPSEM   =   corresponds to the HPS EM

LPS   =   corresponds to the LPS

LPSEM   =   corresponds to the LPS EM

norm   =   normalized value

SP   =   set-point value

TCT   =   corresponds to the tail cone thruster

trans   =   corresponds to the transient power command

Acronyms and Abbreviations

AC   =   Alternating Current

APU   =   Auxiliary Power Unit

CRZ   =   Cruise

DC   =   Direct Current

EAP   =   Electrified Aircraft Propulsion

EM   =   Electric Machine

EM1   =   Electric Machine 1 – derives its power from GTF1

EM2   =   Electric Machine 2 – derives its power from GTF2

ESD   =   Energy Storage Device

FAA   =   Federal Aviation Administration

GTF   =   Geared Turbofan

GTF1   =   Geared Turbofan 1

GTF2   =   Geared Turbofan 2

HPC   =   High Pressure Compressor

HPS   =   High Pressure Spool

IWP   =   Integral Wind-up Protection

LPC   =   Low Pressure Compressor

LPS   =   Low Pressure Spool

NPSS   =   Numerical Propulsion System Simulation

PEx   =   Power Extraction

PI   =   Proportional Integral

SLS   =   Sea Level Static

SP   =   Set-Point

SS   =   Steady-State

STARC-ABL =   Single-aisle Turboelectric AiRCraft with Aft Boundary Layer propulsor

TCT   =   Tail Cone Thruster

T-MATS   =   Toolbox for Modeling and Analysis of Thermodynamic Systems

TEEM   =   Turbine Electrified Energy Management

I. Introduction

Electrified aircraft propulsion (EAP) covers a vast range of possible propulsion system architectures. Those of particular interest are systems that integrate an electric power system with turbomachinery to create a hybrid system. The result is a more expansive and complex propulsion system. While the new architecture offers several benefits, it also introduces more failure modes and a greater possibility of failures occurring due to the added complexity and number of components. The propulsion system is also highly coupled such that the failure of one component could have a cascading effect throughout the rest of the system. These possibilities raise concerns for system safety and deserve investigation. The study presented in this paper seeks to investigate the failure modes of an EAP concept propulsion system and to demonstrate the ability to mitigate failures through reversionary control modes.

The presence of an electrical power system that interfaces with the spools of turbomachinery through electric machines (EMs) enables the use of the Turbine Electrified Energy Management (TEEM) concept, which is a control strategy for propulsion systems with electrified turbomachinery, first introduced in Ref. [1]. TEEM seeks to improve operability to enable benefits for the turbomachinery that ultimately benefits the vehicle it propels. For instance, the ability to tightly control operability metrics and limit off-design operation of the turbomachinery during transients will alleviate constraints on the engine design and could result in improved performance. It may also help to make the engine lighter and shorter in length.

Figure 1. STARC-ABL visual representation

Many EAP concepts include much of the electrical hardware needed to implement TEEM and obtain its benefits. This study examines the application of TEEM to one such EAP concept and investigates some associated failure mitigation techniques for maintaining the operability benefits of TEEM in the event of various failures. In theory, the engine design can take advantage of the operability benefits enabled by TEEM to achieve better performance with less operability margin. Therefore, it is important to retain the operability benefits of TEEM during failures so that engine transients can be confidently handled without operability issues. Alternatively, the transient control logic would need to further limit the acceleration and deceleration rates of the engine to mitigate possible transient operability issues. Increasing thrust response time could limit the ability of the aircraft to respond in emergency situations, creating an undesirable safety concern.

This study explores the control-based mitigation of a variety of EAP failure scenarios. The application is to the Single-aisle Turboelectric AiRCraft with Aft Boundary Layer propulsor (STARC-ABL) [2], depicted in Fig. [1]. STARC-ABL is a NASA-developed conceptual single-aisle commercial transport with an electrified propulsion system. Figure 1 shows a visual representation of the aircraft. The concept has two wing-mounted engines and an aft boundary layer ingesting tail cone thruster (TCT) at the back of the fuselage. The TCT is driven by electric motors that derive their power from the wing-mounted engines.

The study presented here is not exhaustive but does address the failure of major components within the propulsion system. This includes independent failures of an engine variable bleed valve (VBV), an engine variable area fan nozzle (VAFN), the electric machine integrated with the high pressure spool (HPS), the electric machine integrated with the low pressure spool (LPS), one of the parallel power systems, an entire engine, and the TCT. The Federal Aviation Administration Advisory Circular 25.1309-1A [3] requires that there shall be no single aircraft failure that will result in a catastrophic condition in which multiple fatalities or loss of the aircraft are expected. The Federal Aviation Administration (FAA) also requires that subsequent failures during the same flight should be assumed unless the probability is extremely low. The set of independent failures chosen in this study begins to consider these requirements for an EAP concept vehicle.

This study has similarities to Ref. [4] which also used STARC-ABL as the basis of its study. There are several key differences. Ref. [4] did not include the TEEM concept. It only considered a subset of failure scenarios which were independent failures of the engine, the TCT, and the power systems interfacing each engine to the TCT. There are also differences in the high-level control strategy and the mitigation techniques employed to address failures. For example,

Ref. [4] attempted to achieve thrust symmetry in the steady-state (SS) and dynamic response of the engines, as applicable. In this study, the goal was to maintain as much thrust as possible, even if it results in asymmetric thrust.

The rest of the paper is organized as follows. Section II provides background about the STARC-ABL concept and the model used in this simulation study. Section III discusses the general control approach that includes TEEM implementation. Section IV provides more details about the TEEM control strategy and discusses how it is applied to the STARC-ABL. Section V describes the failure mitigation strategies and documents results from the study for the various failure scenarios. Finally, Section VI provides some concluding remarks.

II. The STARC-ABL Propulsion System

The STARC-ABL propulsion system consists of two wing-mounted engines and an aft boundary layer ingesting TCT that is driven by two electric motors. The system is represented with a schematic in Fig. 2. The geared turbofans (GTFs) are denoted in the figure as GTF1 and GTF2. Generators attached to the low pressure shaft (LPS) of each engine extract power that drives the motors that spin the TCT. Between the generators and motors, rectifiers convert electrical power from alternating current (AC) to high voltage direct current (DC) for power transmission at high voltage to reduce the cable diameter and weight. The power is converted back to AC through inverters before being applied by motors attached to the TCT shaft. EMs are also present on the high pressure shaft (HPS) of each engine for the primary purpose of extracting power to meet the power demands of the aircraft systems.
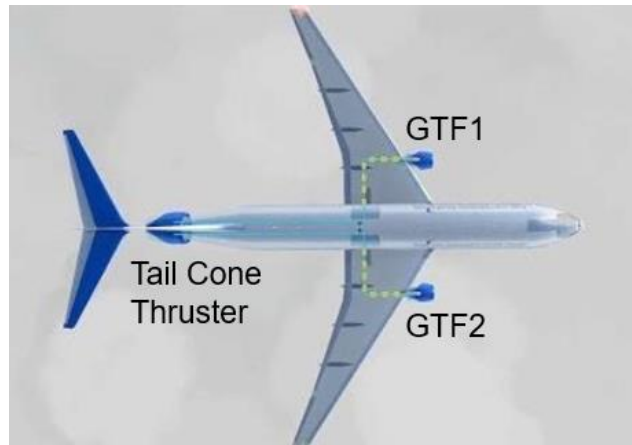
Figure 2. STARC-ABL propulsion system

It could also serve a role in engine starting and will be leveraged in the implementation of the TEEM control strategy. TEEM will also require the addition of energy storage for both engines. Energy storage devices (ESDs) will be connected to the DC bus of each power system. In this study, the ESDs will be given a total energy capacity of 8 kW-hr. The LPS and HPS EMs have peak power capabilities of 2500 hp and 500 hp respectively. Each of the two motors on the TCT has a peak power limit of 1900 hp. The EMs are assumed to have an efficiency of 96% and the inverter/rectifier power electronics are assumed to have efficiencies of 99%. A high-level representation of the STARC-ABL propulsion system is shown in Fig. 3.

The engines have various control inputs. The engine power level is controlled by the fuel flow rate (W_f). Each engine and the TCT have a VAFN to promote fan operability. Each engine has a VBV to promote Low Pressure Compressor (LPC) operability. The engines also have variable stator vanes, but their operation is captured within the high pressure compressor (HPC) performance map that defines the HPC performance. Therefore, there is no ability within the model to alter the variable stator vane input.

An auxiliary power unit (APU) is not included in this study for a few reasons. First, it is normally located in the rear section of the fuselage where the TCT now resides. Second, its existence is not mentioned in the description of the STARC-ABL concept. Third, the engines and TCT have very capable EMs that could perform the duties of the APU. With the increasing electrification in aircraft and their propulsion systems, the authors assume that energy storage will be available to start the engines and run necessary aircraft systems on the ground prior to and after a flight. Finally, assuming that an APU is not available to supply additional power in the event of failure scenarios leads to a more conservative assessment of the robustness of the propulsion system to failures. In such a case, any failure of a component that results in a loss of power extraction (PEx) to support the aircraft systems power demand would require power to be reallocated from the working portions of the system to meet the demand of the aircraft systems. This will mean a reduction in the maximum power that could go to the TCT.

The propulsion system model was originally developed using the Numerical Propulsion System Simulation (NPSS) code [5]. A new model of the system that is more amenable to dynamic simulations and control development was created using a MATLAB/Simulink[TM] based library developed at NASA called the Toolbox for Modeling and Analysis of Thermodynamic Systems (T-MATS) [6]. T-MATS and its solver work similar to NPSS, but, unlike NPSS T-MATS is built on the Simulink graphical block diagram development environment. Both codes simulate the engine cycle and model each component with thermodynamic processes. Turbomachinery component performance is
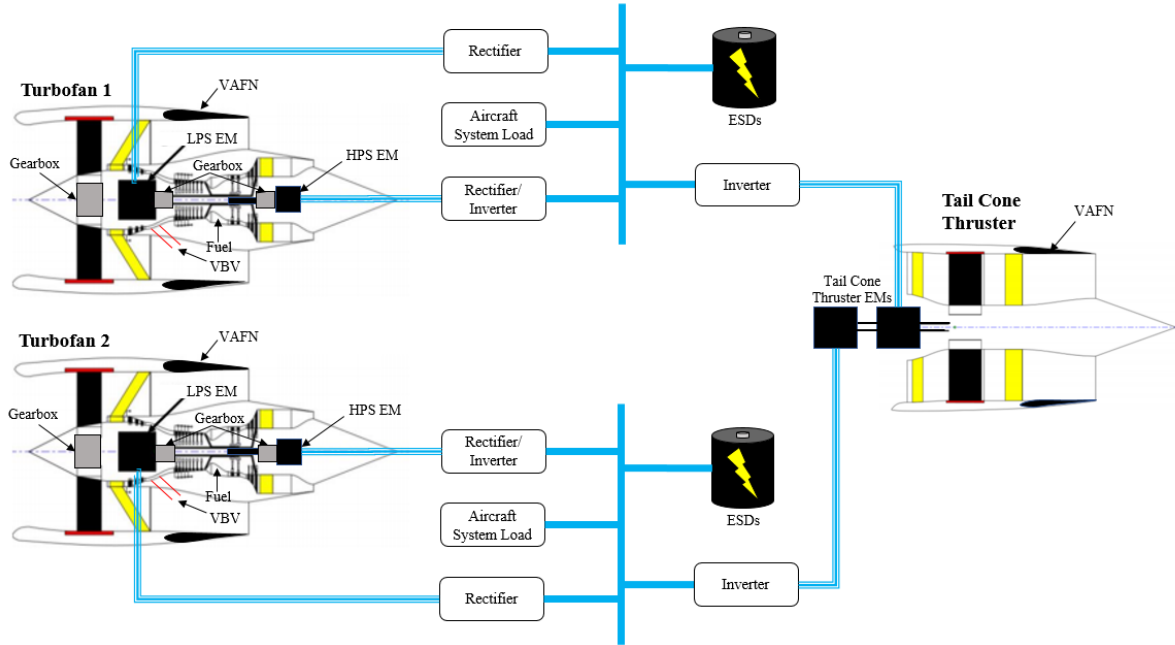
Figure 3. Representation of the STARC-ABL propulsion system

modeled with performance maps that relate performance variables like pressure ratio and efficiency to operating values such as corrected shaft speed and corrected mass flow rate. Components are linked together and parameterized to construct an entire propulsion system. An iterative solver is used to satisfy the governing physics at each time-step. Shaft dynamics are captured using a fixed time-step ordinary differential equation solver in Simulink. T-MATS is used to model both engines and the TCT. The electrical power systems are modeled simplistically by calculating losses through each component based on the constant efficiencies mentioned earlier.

Given the variety of failure modes tested in this study, it would be an extensive and cumbersome effort to address and evaluate failure mitigation strategies for the entire flight envelope and power range. Therefore, this study focuses only on the entire power range for sea level static (SLS) conditions (Altitude = 0 ft, Mach number = 0, standard atmospheric conditions) and cruise (CRZ) conditions (Altitude = 37,000 ft, Mach number = 0.785, standard atmospheric conditions). Thus, the model was modified to simulate failures for these select cases.

III. Baseline Controller

The two turbofans and the TCT must be coordinated through the control system. The engine power levels must be regulated through control of the fuel flow rate, while the VBV and VAFN schedules must be employed to achieve acceptable LPC and Fan operability margins throughout the operating range of the engine. The power applied by the motors on the TCT shaft must be met by the power extracted from the GTFs and achieve the desired TCT thrust. A high level view of the flow of information between the different components of the model is illustrated in Fig. 4. As can be seen, the engine controllers and TCT controllers share information to remain coordinated such that power extraction from the GTFs is consistent with the power demand of the TCT, and the overall desired thrust is achieved.

The baseline engine controller logic associated with each GTF is represented at a high level in Fig. 5. It consists of controllers for the fuel flow rate W_f, VBV, VAFN, and torques applied by the EMs on each spool (τ_{LPSEM} and τ_{HPSEM}). The controller demands are denoted with the subscript dmd. Note that outputs from the fuel flow controller and the TCT controller are shared with the EM controllers.

The nominal fuel flow rate command for each engine is generated by a Proportional Integral (PI) controller with integral windup protection (IWP). It seeks to achieve a desired corrected fan speed. The fan speed set-point (SP) is a function of the power level angle (PLA), which refers to the angle of the throttle lever controlled by the pilot. The overall thrust varies linearly with PLA. In addition to the nominal fuel flow controller, several limit controllers have been added to ensure that the engine operates within pre-defined limits. This includes maximum limiters for the turbine inlet fan speed (N_{fan}), HPS speed (N_{HPS}), temperature (T_4), static HPC discharge pressure (p_{s3}), and acceleration. Minimum limiters for p_{s3} and deceleration are also included. Each of the limit controllers have associated SPs. While T_4 is not measurable with current flight-quality sensors, it was easier to directly use T_4 in this purely conceptual study
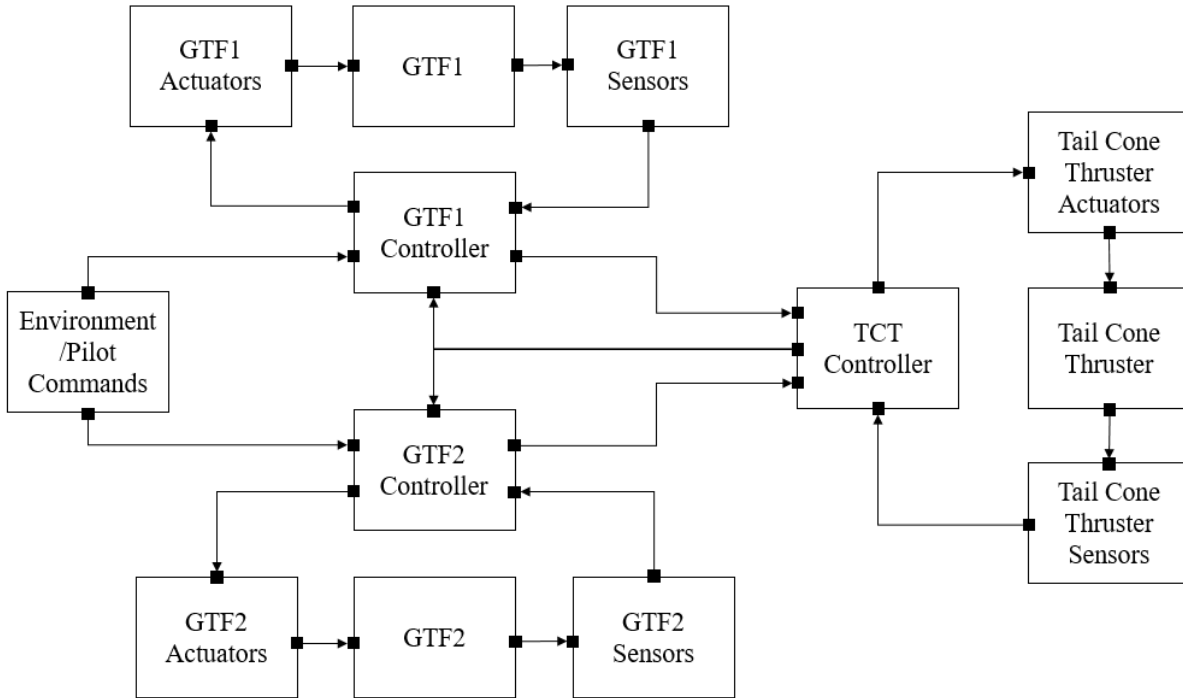
Figure 4. Schematic of the flow of information in the overall model

rather than to use a proxy measurement. The acceleration and deceleration limiters were implemented in a manner similar to that in Ref. [7], [8], and [9]. Specifically, the fuel flow rate is directly limited. This simplified approach limits the change in fuel flow command from one time step to the next. Essentially it defines a maximum and minimum ramp rate for the fuel flow that is chosen to achieve a desired thrust response time. Given the numerous failure scenarios to be tested, it was much simpler to employ this limit logic than to create acceleration and deceleration schedules for both engines for each failure scenario and for the SLS and CRZ conditions of interest. Apart from the acceleration and deceleration limiters, all other limit controllers utilized PI control logic with IWP. A Max-Min control logic approach was taken when selecting which controller to use. The nominal controller command was compared with the commands of all the maximum limiters and the minimum value was chosen. That value was compared with the commands of the minimum limiters and the maximum value was chosen to be the command issued to the fuel metering valve. A simple visualization of this logic is depicted in Fig. 6.

The engine VBV and VAFN utilize schedules to determine their commands. The schedules are functions of the corrected fan speed. The VBV schedule was constructed from steady-state data to maintain a minimum LPC stall margin (SM) and the VAFN schedule was constructed from steady-state data to maintain a defined r-line on the fan performance map. In this instance, the first and highest r-line of the performance map is assumed to be the stall line. The r-lines run parallel to one another and do not intersect. Thus, maintaining a selected r-line will maintain some distance away from the stall line on
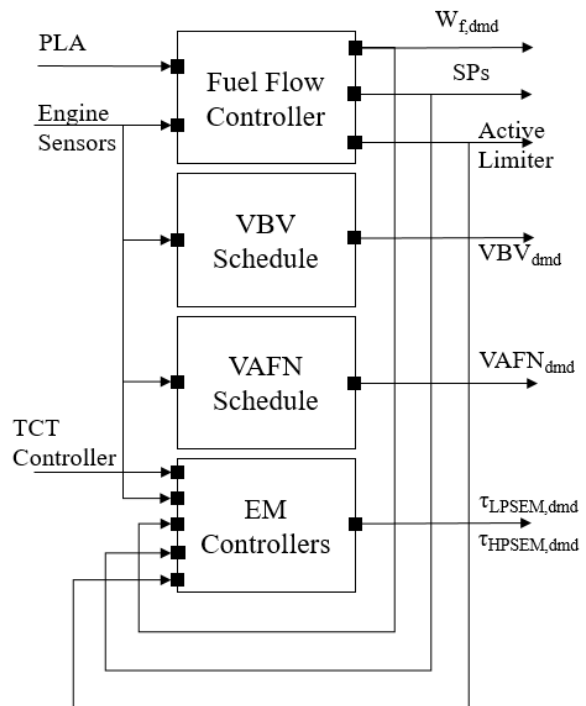
Figure 5. High level block diagram of the baseline GTF controller
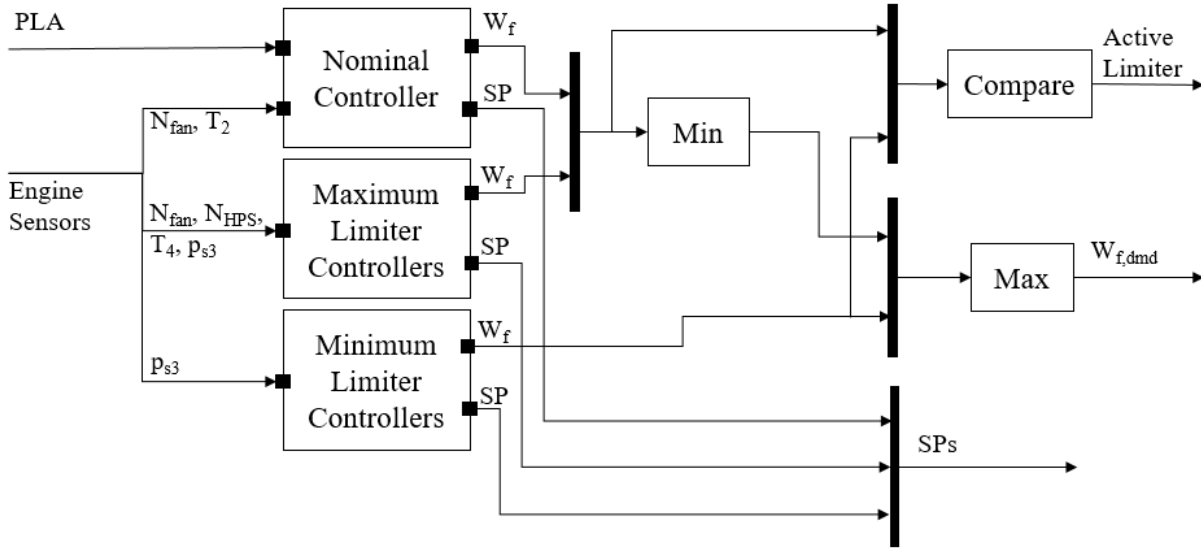
Figure 6. High level block diagram of the fuel flow controller logic

the performance map. In the solution of the governing equations of the engine model, the fan r-line is an independent variable that is adjusted by the solver. R-lines are useful for this purpose because they promote a unique solution within the potential solution space of compressor maps where a single compressor corrected speed and pressure ratio can be associated with two different corrected flow rates.

The EM controller commands consist of nominal and off-nominal components. The TEEM controllers will command a net power input to, or extraction from, the engine spools relative to the nominal power extraction required to power the TCT and aircraft systems. A high level depiction of the control logic power management control strategy is shown in Fig. 7. Note that more details are provided about the TEEM (off-nominal) control logic in the next section. The major inputs to the controller include: the TCT power command and power split between the two engines, the engine sensor data, the fuel flow command, the fuel flow controller set-points, and the active fuel flow controller. The fuel flow command is used to determine the EM controller set-point command while information about the fuel flow set-point and active controller is utilized to determine the transient state of the engine in order to decide if the TEEM control logic should be active or inactive. The ESD supplies additional power for injection and can absorb excess power during extraction. Therefore, during each transient, the state of charge (SOC) of the ESD will change. A nominal power controller is present for each ESD to modify the nominal power extraction command in-order to drive the SOC to its desired value. The controller is a PI controller with constant gains that also has a feedforward component. Information about the power demands of the TCT and aircraft systems is used in the determination of the feedforward component that is added to the output of the PI controllers. The magnitude of the modification to the
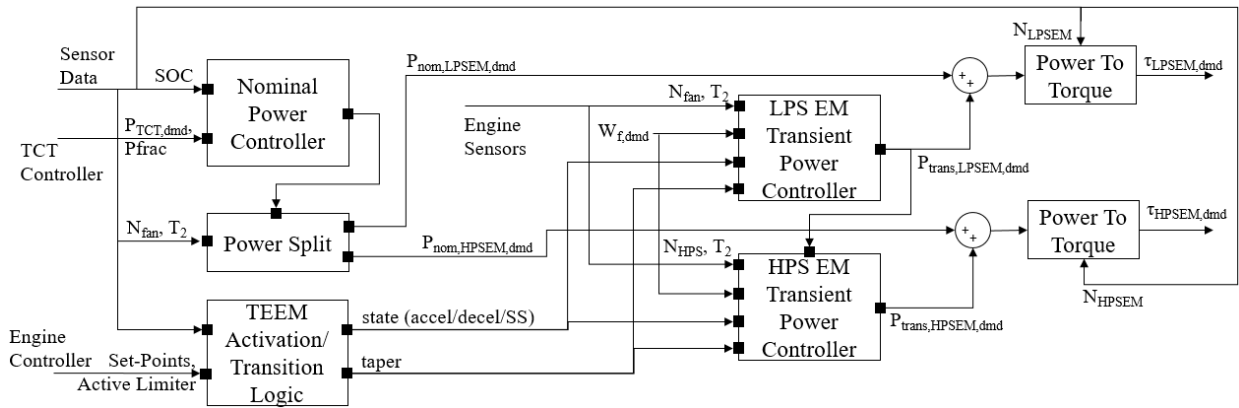
Figure 7. High level block diagram of the electric machine controllers

7
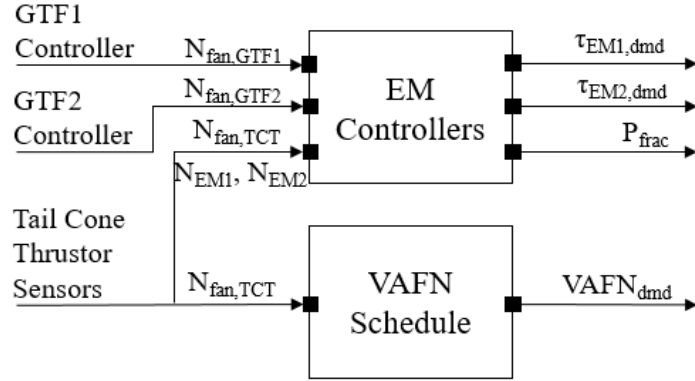
Figure 8. High level block diagram of the TCT controller
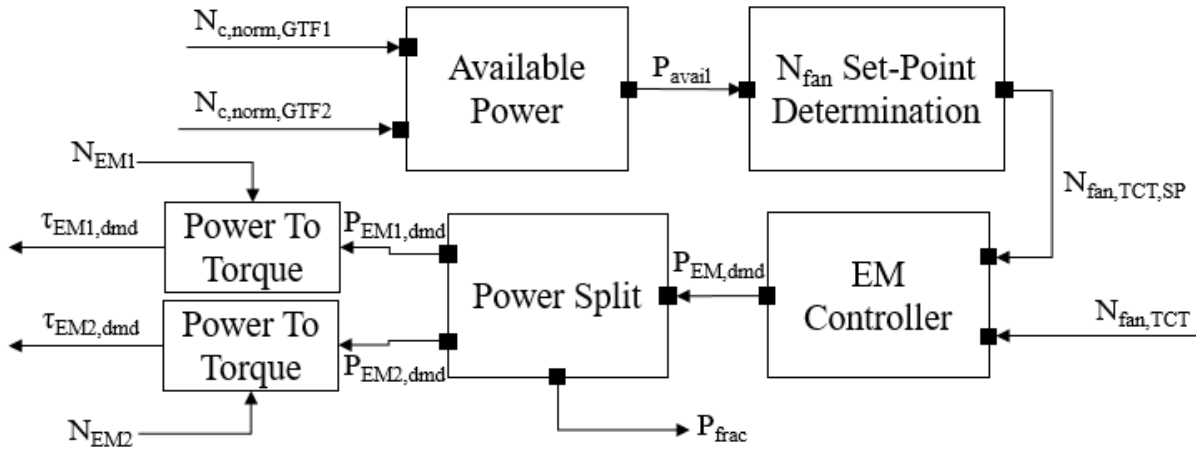
Figure 9. High level block diagram of the power/torque controller for the TCT

nominal power extraction command is limited to 200 hp and the desired SOC is set to be 80%. In addition to charging the ESD, this controller also assures that all the electrical power generated by the engine is consumed by the TCT and aircraft systems during steady-state operation. The nominal power extraction command is split between the LPS and HPS EMs according to a schedule. The HPS EM power fraction is a function of the corrected fan speed and the LPS EM extracts the remainder of the power demand. The power schedule was designed to maintain ~350 hp of electrical power generation from the HPS, which is equivalent to the nominal aircraft power system demand from each engine and is consistent with the original STARC-ABL concept. The TEEM controller commands, labeled $P_{trans,LPSEM,dmd}$ and $P_{trans,HPSEM,dmd}$ in the figure, are added to the "nominal" commands for each electric machine. The final power commands are converted to torque commands by using speed sensor feedback from the LPS and HPS EMs.

The TCT has two inputs. One is a VAFN which is scheduled as a function of the TCT's corrected speed. The other is the total amount of electrical power applied to the TCT shaft via the EMs. These inputs are shown in Fig. 8. To determine the power demand, several steps are performed, as illustrated in Fig. 9 . The corrected fan speed of each turbofan is converted to a normalized value, $N_{c,norm}$, that exists on a scale between 0 and 1 where 0 corresponds to idle and 1 corresponds to maximum power. This value is used to determine how much power can be supplied to the TCT by interpolating from a lookup table. The available power, P_{avail}, from both engines is summed and then fed into a schedule that determines the TCT's corrected speed set-point. A PI controller with IWP is used to command the power to achieve the set-point corrected speed. The power command is split between the two EMs on the TCT shaft based on the electrical power that can be supplied by the turbofans that they interface with through their respective power systems. In the absence of failures, there is a 50/50 power split between the two turbofans and power system strings.

IV. TEEM Transient Operability Control

TEEM is a control concept that leverages electrical hardware to influence the operation of the turbomachinery with which it is interfaced. Most notably, prior studies [1,7,8,9,10] have investigated the use of TEEM to substantially

improve transient operability. To be explicit, transient operability is referring to the trade-off between engine responsiveness and stability, primarily compressor stability. Specifically, this means accelerating and decelerating the engine shafts to change thrust production while maintaining adequate stall margin in the compressors to guarantee stability. Transient operability is improved by using EMs to supplement torques to the engine spools during transients such that it keeps the turbomachinery components operating closer to their steady-state operating conditions without sacrificing responsiveness. Typically, during transients, mismatches in flow and speed conditions within the engine produces off-incidence flow in the turbomachinery components, most notably the compressors. The off-incidence flow relative to the compressor blades can lead to the undesirable conditions of stall and/or surge. For this reason, the engine design is constrained by the need to add significant operability margins at the expense of performance. Ref. [11] outlines some of the design considerations there are for turbomachinery and how operability constraints can impact performance. With the ability to tightly regulate the operability of the engine by using the electrical power system, it opens the design space for the engine. In this effort, a re-design of the STARC-ABL turbomachinery is not attempted, but performance improvements would be expected if such an effort was taken. In this study, a TEEM control strategy is employed and reversionary control approaches attempt to retain the operability benefits that are promised by TEEM when failures are encountered.

Prior applications of TEEM have considered a standalone turbofan engine, a single spool turboshaft engine meant for power production to drive external propulsors, and an augmented parallel hybrid turbofan in which a motor on the LPS is used to input power on that shaft to augment the thrust produced by its fan. In all these cases, the same observations were made about the general effectiveness of adding and extracting power on each shaft with respect to compressor operability metrics such as SM. Generally, power addition on both spools is helpful to better maintain steady-state relationships during acceleration transients. However, only power addition on the HPS was found to be effective at improving HPC operability. Generally, power extraction from the LPS and power addition on the HPS is helpful with respect to compressor operability during decelerations. Given these observations, the EM attached to the HPS has been used to apply power during both accelerations and decelerations while the EM on the LPS has typically been used only to extract power during decelerations. To minimize the use of energy, eliminate the need to dissipate energy, and reduce the power requirement of the LPS EM needed to implement TEEM during transients, a power transfer solution is recommended in which the power extracted from the LPS is applied to the HPS. The controllers are implemented as proportional integral (PI) controllers that seek to maintain a steady-state operating relationship with respect to fuel flow rate. The same approach is taken in this study. Similar to the prior control implementations [7,9,10], logic is also present to activate/deactivate a TEEM controller so that it is only active during transients. This involves sensing if the engine is accelerating, decelerating, or neither and is referred to in the TEEM control logic as the engine "state".

Application of TEEM to STARC-ABL demanded some changes to the control strategy described above due to the nature of how STARC-ABL operates. This application was the first instance in which TEEM was applied to an engine with large-scale power extraction from the LPS of a turbofan engine that also produces thrust. Due to the large amount of power extraction from the LPS, it is overpowered and oversized compared to the LPS on a standalone engine meant to produce the same amount of thrust. This translates to a larger LPS inertia with respect to the HPS. Although not a perfect comparison, the ratio of LPS to HPS inertia of the STARC-ABL engines is 12.8 compared to 9.4 for the advanced geared turbofan that was used in Ref. [7] and [8]. It can also be noted that the STARC-ABL engine produces less thrust than the engine in Ref. [7] and [8]. As the engine accelerates, the amount of power extracted from the LPS increases substantially and this causes the need to add more fuel in order to accelerate the LPS as the engine is commanded to increase its thrust production. The increasing power extraction on the LPS could be viewed as representing an increasing spool inertia that resists the increase in speed. All these factors exacerbate the operability issues that occur during acceleration transients, which result in the need to apply power to the LPS, larger power requirements for the EMs, and larger energy and power requirements for the ESDs. During deceleration transients, the power extraction is decreased, which can be viewed as power addition on the shaft in a relative sense. Given that the goal is to slow down the LPS faster in order to reduce the lag between the change in shaft speed and the change in fuel flow rate, the decreasing power extraction from the LPS effectively off-loads the shaft and makes it more difficult to reduce the speed which is counterproductive for achieving this goal. This situation provides a plausible explanation for why the LPC operability in this application was observed to be worse than prior applications of TEEM during decelerations and why more power extraction from the LPS and or power injection to the HPS was required.

Initially, the control strategies employed in Ref. [7] were used for this application, but the degree to which it impacted transient operability was less than desirable. To improve the HPC SM response during transients, power was applied to the LPS through the LPS EM and power was supplied by the HPS EM to the HPS. The LPS EM controller attempted to achieve the steady-state LPS speed vs. fuel flow relationship while the HPS attempted to achieve the steady-state HPS speed vs. fuel flow relationship. During decelerations, the LPS EM would become saturated because

it is primarily sized for power extraction to drive the tail-cone thruster. It was viewed as undesirable to further increase the size of the power system to accommodate TEEM. Therefore, the HPS EM could apply more power to the HPS during decelerations which enabled a non-zero power solution. However, it should be noted that the ESD energy was only reduced during decelerations in a few failure scenarios. The LPS EM still had the objective to better match the steady-state LPS speed vs. fuel flow relation and the HPS EM had the objective to better match the steady-state LPC stall margin vs. fuel flow relationship. It is recognized that the LPC SM is an undesirable control variable due to the need of a model and potentially an estimator, and concern over the accuracy and computational challenges associated with their use. However, the objective of this study is simply to demonstrate capabilities, rather than to provide a completely practical control approach. The described changes in control strategy greatly improved operability without the need to increase EM sizes, though they may also increase power and energy requirements for the ESDs. It should be noted that the control approach taken here is not optimal. However, the controllers are sufficient to demonstrate the TEEM concept and the reversionary control strategies presented in this paper.

V. Failure Scenarios and Mitigation Strategies

Several failure scenarios and mitigation strategies are evaluated. In each failure case, the failure is assumed to be correctly detected and reversionary control logic is activated to mitigate the failure. The actual event of the failure is not simulated, only the operation after the fault has been detected. At that point, it is assumed that the reversionary control logic has been activated, and the system has reached a steady operating condition. The reversionary control logic modifies operation of the engines and the TCT, which allows the system to continue to safely operate and produce thrust in the presence of the failure. Note that all component failures considered in this study are applied only to GTF1. GTF2 is not used to simulate failures, but its operation may be altered to help mitigate failures occurring elsewhere in the propulsion system. For instance, if GTF1 is restricted in its ability to supply power to the aircraft systems and
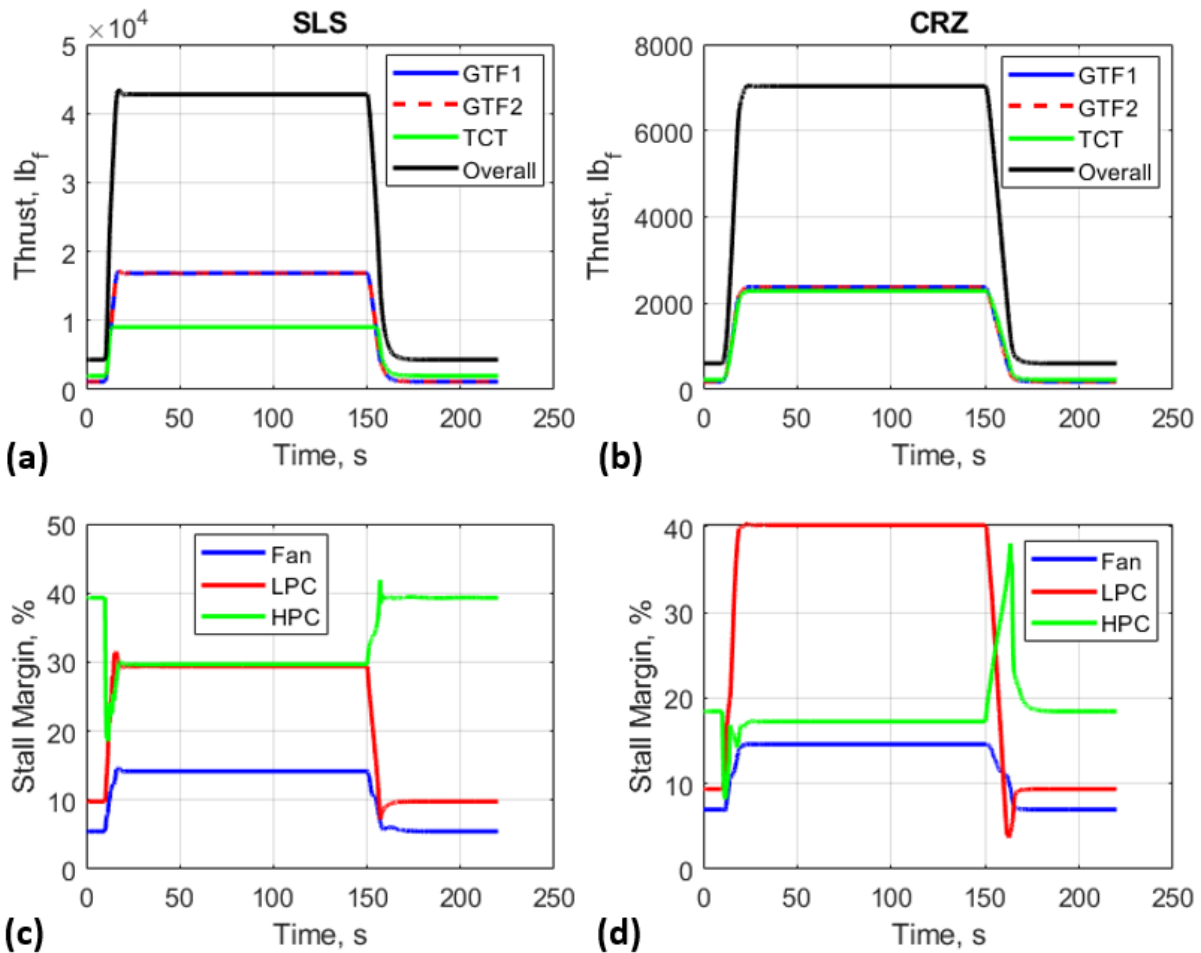
Figure 10. Thrust and stall margin response of the nominal engine without TEEM.

TCT, the power extracted from GTF2 and allocation of that power could be modified. Any change in power extraction could also be accompanied by changes in actuator schedules. All the simulation scenarios consider a burst and chop transient PLA input in which the throttle starts at idle, abruptly increases to full power, and later is abruptly reduced back to idle. This input allows the performance and operability to be evaluated at low and high power operating conditions as well as during both acceleration and deceleration transients. Figure 10 shows burst and chop responses for the baseline model (without failures). For the same powertrain configuration and transient, Figure 11 shows the fuel flow rate, VBV position, GTF VAFN area, TCT VAFN area, HPS EM Power, LPS EM Power, TCT Electric Machine 1 (EM1) Power, and TCT Electric Machine 2 (EM2) Power. These results provide a basis of comparison with the following failure scenarios: VBV failure, engine VAFN failure, HPS EM failure, LPS EM failure, power system failure, GTF failure, and TCT failure. The following paragraphs will describe each of the aforementioned failure scenarios and the measures taken to mitigate them.

The VBV is designed to fail open. This occurrence will degrade the performance of the engine by unnecessarily bleeding worked air from the core, but it will result in more favorable operability. In the simulation, the VBV is fixed to its fully open position. The VBV position is expressed numerically as the fraction to which the valve is open, where 1 is fully open and 0 is closed. The GTF1 VAFN schedule was adjusted to correct any shift in the fan operating line. The fuel flow rate and EM torque controllers set-point schedules and gain schedules were redesigned to be consistent with the shift in engine performance. Operation of GTF2 remained the same, as did the power extraction schedules and the operation of the TCT.

VAFNs are potential advanced features of future high bypass turbofans. VAFNs are not commonplace and thus, the fail-safe behavior of such actuators is not well-defined. Ideally, it would be simplest to fail the VAFN into its minimum or maximum area position. However, there is an issue with this approach because the VAFN area varies so much and the trends do not remain the same. For instance, at SLS conditions, the VAFN area needs to increase as the fan speed decreases and the opposite is true for CRZ conditions. This is illustrated in Fig. 12 which plots the VAFN schedule for SLS and CRZ to maintain the same operating line. Increasing the VAFN area is favorable to the fan stall margin in either case, but there is a limit. Increasing the VAFN area too much can push the operating point on the fan map off the bottom of the map which would choke the fan. If the VAFN area is too small, there may not be enough
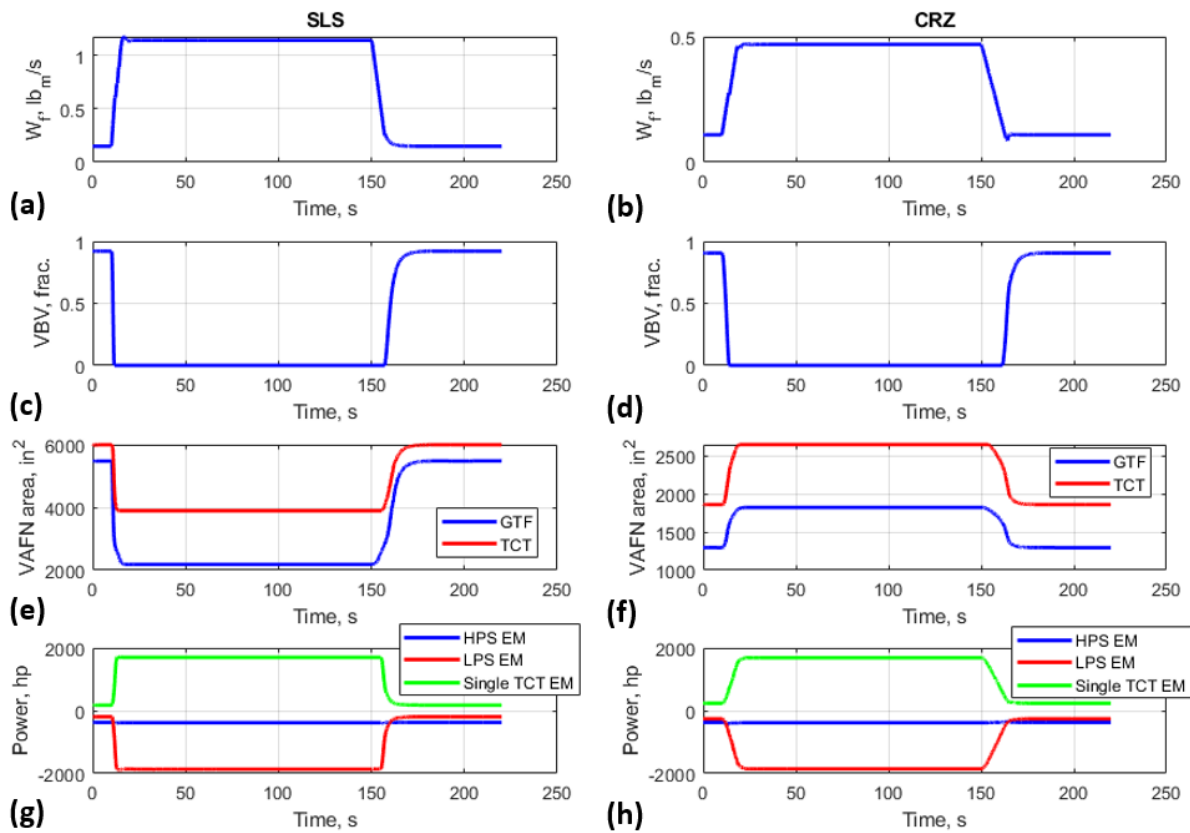
Figure 11. Inputs for the nominal system without TEEM

operability margin and the fan may stall or surge. This makes the choice of a fail-safe position difficult because the maximum area (~5500 in^2) will choke the fan and the minimum area (~1200 in^2) will stall or surge the fan. Thus, an intermediate fail-safe position of 2100 in^2 was chosen. The details of how this fail-safe behavior would be implemented were not addressed but assumed to be possible. The change in the VAFN area significantly reduced the maximum thrust at CRZ conditions due to choking limits, and the minimum thrust at SLS conditions due to stall margin limits. The GTF1 VBV schedule was adjusted to correct for any shift in the LPC operating line. The fuel flow rate and EM torque controllers set-point schedules and gain schedules were redesigned to accommodate the shift in engine performance. The power

Figure 12. Nominal VAFN Schedule

extraction schedules and the operation of GTF2 and the TCT remained unchanged.

Failure of the HPS EM of GTF1 results in the loss of power extraction capability which supplies half of the power required to meet the aircraft systems load demand. Therefore, there is a need to change the power extraction schedules and how the power is allocated for use. It also eliminates the ability to use the HPS EM of GTF1 to impact the transient operability of the engine, thus requiring changes in the TEEM control strategy. The TCT power is reduced to retain the power needed to meet the demand of the aircraft systems. The power fraction split between GTF1 and GTF2 is adjusted to be proportional to the power extraction capability of each engine. The nominal power extraction from GTF2 is modified as the power level of the engine decreases, which called for adjustments in the control schedules of GTF2, including the VBV and VAFN schedules, as well as the set-point and gain schedules of the fuel flow and EM controllers. The adjustment is required because GTF2 produces a larger portion of the electrical power at low power conditions than it normally would. The GTF1 VBV and VAFN schedules were adjusted to respect the same LPC SM and Fan SM limits as the nominal engine. The GTF1 fuel flow and EM controller set-points and control gains were re-designed to be consistent with the shift in engine performance. Due to the reduction of power extraction from GTF1, the GTF1 thrust was able to be increased with the same engine limits. It should be noted that the shafts speed limits were based on failure scenarios and not the baseline engine, and thus the assumption is that the design of the rotating components accounts for the increased speeds encountered during failures of the EMs. The TEEM control strategy

(a)   (b)
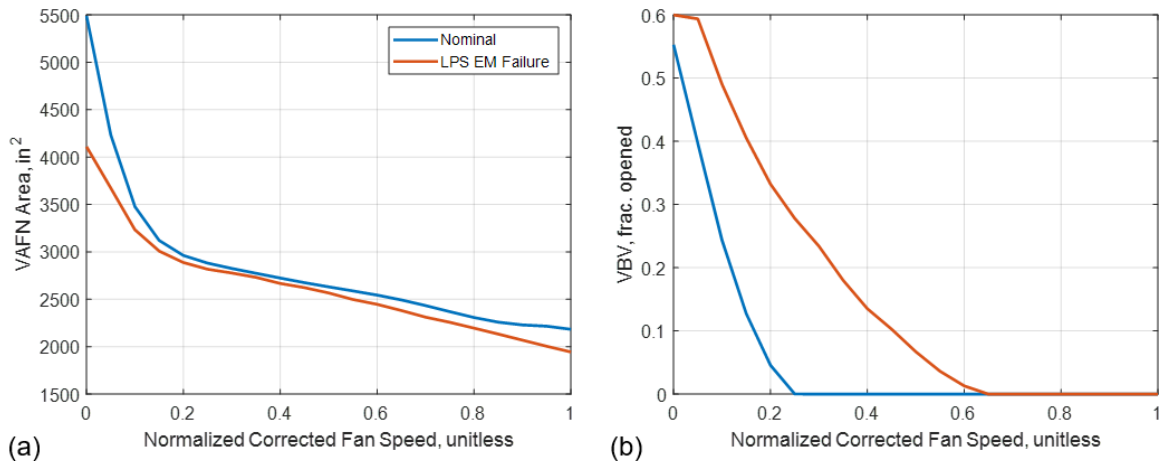
Figure 13. Example of adjustments to reversionary control schedules. Reversionary control adjustments to the VAFN and VBV schedules are shown for a failure of the LPS EM at SLS conditions.

12

remained the same except the GTF1 HPS EM was unavailable for use, which resulted in degraded operability benefits during transient, particularly during accelerations.

Failure of the LPS EM of GTF1 would result in the loss of its power extraction capability, which normally supplies half of the power requested by the TCT. Therefore, there is a need to change the power extraction schedules. Specifically, the TCT power is reduced to reflect the new power extraction capability and the power fraction split between GTF1 and GTF2 is adjusted to be proportional to the power extraction capability of each engine. Similar to the case of a HPS EM failure, the GTF1 and GTF2 controller schedules, set-points, and gains were adjusted to be consistent with the changes in power extraction. An example of this is shown in Fig. 13 for the GTF1 VBV and VAFN schedules. With less power extraction, the maximum thrust of GTF1 was significantly increased, with the understanding that mechanical design constraints were assumed to consider the increase in shaft speeds. The loss of the LPS EM of GTF1 also means that it will not be able to assist with transient operability control, which is expected to result in the degradation of the transient operability benefits promised by TEEM. The control strategy of the HPS EM remains the same.

Failure of the power system of GTF1 could be viewed as any failure that manifests in a way that renders that entire power system useless. For instance, this could occur in the event that one or more of the cables within the power system were severed. Such a failure would result in the loss of power extraction from GTF1 for both the aircraft systems and the TCT. It would also eliminate the use of the EMs for the TEEM transient operability control strategy. The TCT power would be derived entirely from GTF2 and the amount of power it receives from GTF2 would be reduced due to the increased demand on GTF2 to supply double the amount of power to support the aircraft systems. Thus, less than half of the power normally available to the TCT would be available. The change in power extraction from the engine calls for re-evaluation of the control schedules, set-point schedules, and gain schedules. The maximum thrust produced by GTF1 increased as a result of the lack of power extraction. However, substantial reductions in transient operability are expected without the modification of acceleration and deceleration limit logic that will significantly increase the response time of the engine.

Failure of GTF1 would share similarities with a failure of the GTF1 power system. From the perspective of GTF2 or the TCT, the failure would look the same. The difference will be that, since GTF1 is inoperable, its thrust production capability is lost as well as its power generation capability.

Failure of the TCT would off-load the LPS of both engines, significantly reducing the power extraction from both engines. Only power extraction for the aircraft systems would remain and that power would be extracted using the HPS EMs. Both GTFs would be operated identically. The control schedules, set-point schedules, and controller gains of the two engines were updated to account for the shift in performance related to the change in power extraction. The maximum thrust of both engines was able to increase, but all thrust production was lost from the TCT.

It should be noted that failure of the TCT VAFN was considered. The same challenges noted for the GTF VAFNs were encountered. Unlike the GTF VAFN, no fail-safe position exists that would keep the operating point on the fan map for both SLS and CRZ. Therefore, a failure of the TCT VAFN was assumed to require shutdown of the TCT and, thus, was treated as a failure of the TCT.

The impact of the failure scenarios on some of the performance and operability parameters of the propulsion system are summarized in Table 1, 2, 3, and 4. Tables 1-4 cover results for GTF1, GTF2, the TCT, and the overall propulsion system, respectively. The first 2 columns of each table show the impact of TEEM, which is evident by the improved LPC and HPC transient stall margin relative to the nominal system without TEEM. During the various failure scenarios, the reversionary control strategies are able to retain most or all the transient operability benefit as is evidenced by the elevated transient SMs and their close proximity to the SS SMs. The maximum and minimum ESD peak power and the amount of energy used during the acceleration and deceleration transient are provided in Table 1 and Table 2. These values provide an idea of the electrical power and energy required to implement TEEM for this application. The one failure case in which reversion control measures cannot be taken to retain the transient operability benefits is the failure of the GTF power system. When this failure occurs for GTF1, there is a relatively large difference in the transient and SS SMs. This outcome stems from the fact that EMs are rendered useless and therefore TEEM cannot be implemented, which renders the GTF1 power system useless. The minimum transient HPC stall margin is still significantly higher than the nominal system without TEEM, but it is also significantly lower than expected. The LPC stall margin of GTF1 reaches a very low value during the deceleration transient. For this failure scenario, it may be necessary to further restrict the acceleration and deceleration rates of GTF1 or to be prepared to shut it down.

Overall, the results demonstrate that the STARC-ABL propulsion system is able to retain a significant portion of its thrust as indicated by modest changes in the maximum thrust. A standard two engine single-aisle aircraft would be expected to lose ~50% of its thrust in the event that an engine is lost and an APU is present to take over the power generation duties. Comparing STARC-ABL to this baseline for comparison, loss of the engine actuators and EMs results in significantly less thrust loss. Of these cases, the greatest thrust loss was in the event of a VAFN failure at

Table 1. Summary results of GTF1 to nominal and failure scenarios in GTF1. The first row for each parameter corresponds to SLS and the second row corresponds to CRZ.

Scenario	Nominal (no TEEM)	Nominal (with TEEM)	GTF1 VBV Failure	GTF1 VAFN Failure	GTF1 HPS EM Failure	GTF1 LPS EM Failure	GTF1 Power System Failure	GTF1 Failure	TCT Failure
ΔMax Thrust, %	0	0	-34.0	+3.8	+2.8	+15.6	+15.6	-100	+18.8
	0	0	-23.0	-63.6	+1.3	+15.2	+8.4	-100	+15.2
Min Thrust as % of nominal Max Thrust	6.9	6.9	6.6	67.6	10.3	10.3	10.3	0	10.4
	8.0	8.0	8.0	8.0	8.0	8.0	8.0	0	12.6
Fan SM, %: Min SS/Transient	5.46/ 5.46	5.46/ 5.34	5.14/ 5.01	5.00/ 5.00	5.68/ 5.59	5.69/ 5.69	5.69/ 5.69	N/A	5.70/ 5.64
	6.96/ 6.82	6.96/ 6.71	7.12/ 6.98	33.35/ 33.29	7.09/ 6.84	7.16/ 7.13	7.31/ 7.27	N/A	8.33/ 7.96
LPC SM, %: Min SS/Transient	9.78/ 7.19	9.78/ 9.07	10.18/ 10.17	14.77/ 14.72	12.51/ 10.71	10.71/ 10.71	12.39/ 5.62	N/A	9.42/ 9.37
	9.36/ 3.65	9.36/ 8.77	12.73/ 12.70	12.57/ 9.43	15.35/ 15.28	10.27/ 9.50	12.50/ 4.29	N/A	8.27/ 8.14
HPC SM, %: Min SS/Transient	29.65/ 18.52	29.65/ 27.63	17.79/ 16.37	29.41/ 28.33	29.38/ 26.94	33.84/ 21.54	33.90/ 21.13	N/A	33.83/ 29.81
	17.23/ 8.17	17.23/ 14.70	12.92/ 10.44	19.22/ 17.58	16.13/ 14.54	34.19/ 23.78	36.77/ 26.98	N/A	24.39/ 22.90
VBV position, frac.: Max	0.922	0.922	1	0	0.329	1	1	N/A	1
	0.907	0.907	1	0.484	0	0.999	0.676	N/A	1
VAFN area, in^2: Max/Min	5490/ 2184	5490/ 2184	5500/ 2439	2100/ 2100	4131/ 2056	4110/ 1948	4096/ 1925	N/A	4112/ 1954
	1822/ 1295	1822/ 1295	1781/ 1310	2100/ 2100	1759/ 1294	1745/ 1325	1749/ 1335	N/A	1745/ 1429
ESD Peak Power, hp: Max/Min	0/0	1816/ -281	1171/ -313	830/ -275	1563/ -282	768/ -48	0/0	0/0	2318/ -267
	0/0	1187/ -290	941/ -276	390/ -161	730/ -256	378/ -48	0/0	0/0	1187/ -297
ESD Energy Usage, kw-hr: Accel/Decel	0/0	1.54/ -0.47	1.03/ -0.51	0.46/ -0.24	1.70/ 0.40	0.80/ 0.59	0/0	0/0	2.07/ -0.37
	0/0	1.19/ -0.64	1.06/ -0.60	0.429/ -0.25	1.40/ 0.40	0.55/ 0.49	0/0	0/0	1.33/ -0.62

CRZ, which totaled 30.7%. Only 11.7% of the thrust was lost in the worst-case event of a single EM (loss of the LPS EM at CRZ), and only 17.5% of the thrust was lost if the power system of one of the engines is lost. Failure of the TCT resulted in a loss of 22.3% of the overall thrust at CRZ. The most significant impact on thrust occurs at CRZ apart from the VBV failure. One scenario of most concern is a failure one of the GTFs. Failure of GTF1 resulted in nearly 50% thrust reduction at SLS conditions and a 54% thrust reduction at CRZ conditions. The greater loss in thrust is believed to be the result of a reduction of available power to the TCT due to the additional load placed on the remaining working engine, which has to supply power to the aircraft that would have been supplied by the engine that failed. This issued could be remedied by using an APU. Another reason for the additional loss in thrust is that the reduction in power to the TCT reduces the aerodynamic benefit of producing thrust in the TCT's low momentum boundary layer ingestion region of the vehicle.

There is a concern over the fail-safe behavior of VAFNs. As can be seen the maximum thrust of GTF1 was reduced by 63.6% during cruise and the minimum thrust was increased to 67.9% of the maximum thrust of the nominal engine for SLS. The operating range of the engine is limited significantly. If there were a demand for a substantial reduction in thrust at SLS conditions, it is likely that GTF1 would need to be shutdown. Failure of the VAFN resulted in the largest thrust reduction for the failure of a single actuator, electric machine, or the TCT, causing a loss of 30.7% of

Table 2. Summary results of GTF2 to nominal and failure scenarios in GTF1. The first row for each parameter corresponds to SLS and the second row corresponds to CRZ.

Scenario	Nominal (no TEEM)	Nominal (with TEEM)	GTF1 VBV Failure	GTF1 VAFN Failure	GTF1 HPS EM Failure	GTF1 LPS EM Failure	GTF1 Power System Failure	GTF1 Failure	TCT Failure
ΔMax Thrust, %	0	0	0	0	0	0	0	0	+18.8
	0	0	0	0	0	0	0	0	+15.2
Min Thrust as % of nominal Max Thrust	6.9	6.9	6.9	6.9	8.4	8.5	8.6	8.6	10.4
	8.0	8.0	8.0	8.0	8.0	8.0	8.0	8.0	12.6
Fan SM, %: Min SS/Transient	5.46/ 5.46	5.46/ 5.34	5.46/ 5.35	5.46/ 5.35	5.60/ 5.51	5.61/ 5.50	5.61/ 5.50	5.61/ 5.50	5.70/ 5.64
	6.96/ 6.82	6.96/ 6.71	6.94/ 6.79	6.96/ 6.71	6.96/ 6.84	6.82/ 6.64	6.72/ 6.51	6.72/ 6.51	8.33/ 7.96
LPC SM, %: Min SS/Transient	9.78/ 7.19	9.78/ 9.07	9.78/ 9.03	9.78/ 9.08	10.89/ 10.88	12.49/ 11.85	12.48/ 11.77	12.48/ 11.77	9.42/ 9.37
	9.36/ 3.65	9.36/ 8.77	12.48/ 11.82	9.36/ 8.77	11.04/ 11.00	12.50/ 11.25	12.77/ 11.32	12.77/ 11.32	8.27/ 8.14
HPC SM, %: Min SS/Transient	29.65/ 18.52	29.65/ 27.63	29.65/ 27.72	29.65/ 27.63	29.65/ 26.79	29.65/ 24.96	29.65/ 24.15	29.65/ 24.15	33.83/ 29.81
	17.23/ 8.17	17.23/ 14.70	15.98/ 14.85	17.23/ 14.70	16.90/ 14.78	15.04/ 13.91	13.37/ 11.88	13.37/ 11.88	24.39/ 22.90
VBV position, frac.: Max	0.922	0.922	0.922	0.922	1	0.723	0.508	0.508	1
	0.907	0.907	0.852	0.907	0.999	0.316	0	0	1
VAFN area, in2: Max/Min	5490/ 2184	5490/ 2184	5490/ 2184	5490/ 2184	4755/ 2184	4734/ 2184	4724/ 2184	4724/ 2184	4112/ 1954
	1822/ 1295	1822/ 1295	1760/ 1295	1822/ 1295	1760/ 1295	1760/ 1295	1760/ 1295	1760/ 1295	1745/ 1429
ESD Peak Power, hp: Max/Min	0/0	1816/ -281	1792/ -281	1773/ -281	1898/ -278	1990/ -277	2046/ -278	2046/ -278	2318/ -267
	0/0	1187/ -290	1091/ -292	1187/ -290	1123/ -288	1036/ -294	992/ -297	992/ -297	1187/ -297
ESD Energy Usage, kw-hr: Accel/Decel	0/0	1.54/ -0.47	1.51/ -0.46	1.47/ -0.44	1.60/ -0.42	1.60/ -0.40	1.61/ -0.38	1.61/ -0.38	2.07/ -0.37
	0/0	1.19/ -0.64	1.16/ -0.58	1.19/ -0.64	1.21/ -0.61	1.14/ -0.58	1.12/ -0.60	1.12/ -0.60	1.33/ -0.62

the thrust at CRZ conditions. The extreme variation of the VAFN made it difficult to find a fail-safe position that worked for SLS and CRZ conditions for a significant portion of the power range of the engine. Also, designing fail-safe behavior to hold the VAFN area at an intermediate value will introduce challenges. With these challenges in mind, it may be worth exploring alternatives to using VAFNs or constraining the engine cycle design by considering the limitation of VAFN and the failure modes they present to the overall propulsion system.

VI. Conclusion

Hybrid electric propulsion will undoubtedly increase propulsion system complexity. An increase in the number of parts will raise the probability of failures while the highly-coupled nature of the turbomachinery and power systems will introduce new modes of failure. This study has begun to consider these failure modes and reversionary control approaches to retain as much performance as possible while maintaining operability, including the transient operability benefits enabled by the Turbine Electrified Energy Management (TEEM) control strategy. Overall, the failure mitigation strategies have demonstrated reasonable capabilities for maintaining operability and thrust under various component failure scenarios. The application to the Single-aisle Turboelectric AiRCraft with Aft Boundary Layer

Table 3. Summary results of the TCT to nominal and failure scenarios in GTF1. The first row for each parameter corresponds to SLS and the second row corresponds to CRZ.

Scenario	Nominal (no TEEM)	Nominal (with TEEM)	GTF1 VBV Failure	GTF1 VAFN Failure	GTF1 HPS EM Failure	GTF1 LPS EM Failure	GTF1 Power System Failure	GTF1 Failure	TCT Failure
ΔMax Thrust, %	0	0	0	0	-6.9	-37.9	-46.5	-46.5	-100
	0	0	0	-28.3	-9.6	-51.8	-62.4	-62.4	-100
Min Thrust as % of nominal Max Thrust	10.0	10.0	10.0	10.0	10.0	10.0	10.0	10.0	0
	8.0	8.0	8.0	8.0	8.0	8.0	8.0	8.0	12.6
GTF1 string motor power, hp: Max/Min	1701/178	1701/178	1701/178	1701/178	1395/162	238/50	0/0	0/0	0/0
	1689/236	1689/236	840/164	1689/236	1388/215	235/66	0/0	0/0	0/0
GTF2 string motor power, hp: Max/Min	1701/178	1701/178	1701/178	1701/178	1668/194	1454/306	1359/356	1359/356	0/0
	1689/236	1689/236	1585/309	1689/236	1659/257	1440/407	1344/473	1344/473	0/0

Table 4. Summary of the overall result to nominal and failure scenarios in GTF1. The first row for each parameter corresponds to SLS and the second row corresponds to CRZ.

Scenario	Nominal (no TEEM)	Nominal (with TEEM)	GTF1 VBV Failure	GTF1 VAFN Failure	GTF1 HPS EM Failure	GTF1 LPS EM Failure	GTF1 Power System Failure	GTF1 Failure	TCT Failure
ΔMax Thrust, %	0	0	-13.4	+1.5	-0.4	-1.9	-3.7	-49.3	-6.4
	0	0	-7.8	-30.7	-2.7	-11.7	-17.5	-54.0	-22.3
Min Thrust as % of nominal Max Thrust	10.1	10.1	10.0	34.1	12.1	12.1	12.2	8.1	8.2
	8.6	8.6	8.7	8.6	8.6	8.7	8.7	6.0	8.5

propulsor (STARC-ABL) prompted changes to the TEEM control strategy used in previous implementations. The current implementation was demonstrated in simulation to significantly improve transient operability. Reversionary control approaches also demonstrated that significant portions of the TEEM operability benefits were retained. Some challenges highlighted by the study include the loss of more than 50% of the overall thrust from a failure of one of the geared turbofans (GTFs) in the propulsion system, lack of practical fail-safe options for the VAFNs, and severely degraded transient operability as the result of complete power system failure. Challenges beyond this study may include quick and accurate identification of the propulsion system failures and the transitioning of the control logic immediately after the failure event.

Acknowledgments

References

[1] Culley, D., Kratz, J., and Thomas, G., "Turbine Electrified Energy Management (TEEM) For Enabling More Efficient Engine Designs," AIAA Propulsion & Energy Forum, Cincinnati, OH. 2018.

[2] Welstead, J. R., Felder, J. L., "Conceptual Design of a Single-Aisle Turboelectric Commercial Transport with Fuselage Boundary Layer Ingestion," AIAA SciTech Forum, San Diego, CA. 2016.

[3] Federal Aviation Administration, "Advisory Circular 25.1309-1A - System Design and Analysis," https://www.faa.gov/regulations_policies/advisory_circulars/index.cfm/go/document.information/documentID/22680, accessed June, 2020.

[4] Simon, D., Connolly, J., "Electrified Aircraft Propulsion Systems: Gas Turbine Control Considerations for the Mitigation of Potential Failure Modes and Hazards," ASME GT2020-16335, ASME TurboExpo, Virtual/Online Conference. 2020.

[5] Claus, R.W., Evans, A.L., Lylte, J.K. and Nichols, L.D., "Numerical Propulsion System Simulation," Computing Systems in Engineering, Vol 2, No. 4, pp 357-364, 1991.

[6] Chapman, J., Lavelle, T., May, R., Litt, J., and Guo, T.-H., "Toolbox for the Modeling and Analysis of Thermodynamic Systems (T-MATS) User's Guide," NASA TM-2014-216638, 2014.

[7] Kratz, J., Culley, D., Thomas, G., "A Control Strategy for Turbine Electrified Energy Management," AIAA Propulsion & Energy Forum, Indianapolis, IN. 2019.

[8] Kratz, J., Culley, D., and Thomas, G., "Evaluation of Electrical System Requirements for Implementing Turbine Electrified Energy Management," AIAA Propulsion & Energy Forum, Indianapolis, IN, 2019.

[9] Kratz, J., Culley, D., "Enhancement of a Conceptual Hybrid Electric Tilt-Wing Propulsion System through Application of the Turbine Electrified Energy Management Concept," AIAA 2021-0875, AIAA SciTech Forum, Virtual Conference, 2021.

[10] Kratz J., Culley, D., "Exploration of the Versatile Electrically Augmented Turbine Engine Gearbox Concept," AIAA Propulsion & Energy Forum, Virtual Conference, 2021.

[11] Philpot, M., "Practical Consideration In Designing the Engine Cycle," Defense Technical Information Center, 1992.